

1 **MOLECULAR CORRELATE OF MOUSE EXECUTIVE FUNCTION. TOP-DOWN**  
2 **and BOTTOM-UP INFORMATION FLOWS COMPLEMENTATION by *Ntng* GENE**  
3 **PARALOGS**

4

5 Pavel Prosselkov<sup>1,2\*</sup>, Qi Zhang<sup>1</sup>, Goto Hiromichi<sup>1</sup>, Denis Polygalov<sup>3</sup>, Thomas J. McHugh<sup>3</sup>  
6 and Shigeyoshi Itohar<sup>1\*</sup>

7

8 <sup>1</sup>Laboratory for Behavioral Genetics, and <sup>3</sup>Laboratory for Circuit and Behavior Physiology,  
9 RIKEN Brain Science Institute, 351-0198 Saitama, Japan

10 <sup>2</sup>Department of Physiology, Faculty of Medicine, Saitama Medical University, Saitama 350-  
11 0495, Japan

12 \*corresponding authors:

13 prosselkov@brain.riken.jp

14 sitohara@brain.riken.jp

15

16 Keywords: executive function, attention and impulsivity, working memory, learning, gene  
17 duplication, cognitive complement

18

19

20 ABSTRACT

21 Executive function (EF) is a regulatory construct of learning and a main characteristic of  
22 general cognitive abilities. Genetic variations underlying the architecture of cognitive  
23 phenotypes are likely to affect EF. Mice lacking one of *Ntng* gene paralogs, encoding the  
24 vertebrate brain-specific presynaptic Netrin-G proteins, exhibit prominent deficits in the EF  
25 control. Brain areas responsible for gating the bottom-up and top-down information flows  
26 differentially express *Ntng1* and *Ntng2*, distinguishing neuronal circuits involved in  
27 perception and cognition. As a result, high and low cognitive demand tasks (HCD and LCD,  
28 respectively) modulate *Ntng1* and *Ntng2* associations either with attention and impulsivity  
29 (AI) or working memory (WM), in a complementary manner. During the LCD *Ntng2*-  
30 supported neuronal gating of AI and WM dominates over the *Ntng1*-associated circuits. This  
31 is reversed during the HCD, when the EF requires a larger contribution of cognitive control,  
32 supported by *Ntng1*, over the *Ntng2* pathways. Since human *NTNG* orthologs have been  
33 reported to affect human IQ (1), and an array of neurological disorders (2), we believe that  
34 mouse *Ntng* gene paralogs serve an analogous role but influencing brain executive function.

35

## 35 INTRODUCTION

36

37 Executive function (EF) is a heterogeneous construct that can be viewed as a set of  
38 processes executively supervising cognitive behaviors (3). EF is an umbrella term for  
39 working memory (WM), attention and impulsivity (AI), and response inhibition, and is  
40 thought to account for the variance in cognitive performance (4). WM, due to its storage and  
41 processing components, is viewed as a bimodal flexible system of a limited capacity. Since  
42 WM maintains current information and simultaneously supports its execution, as a latent  
43 factor underlying intelligence (5), it has been termed as “the central executive” (6) attention-  
44 controlling system dependent on consciousness (7). However an awareness-independent  
45 model has been also proposed (8,9). General learning (Ln) ability depends on attention and  
46 WM interaction (10) as well as perception, the causal and informational ground for the  
47 higher cognitive functions (11). Perception guides our thinking about and acting upon the  
48 world and serves as an input to cognition, via a short-term memory mediated interactions  
49 (12). A possible mechanism linking perception and cognition would be attention (13).

50 Perception (bottom-up) and cognition (top-down) have been historically viewed as  
51 independently operating encapsulating domains. Such embodiment has paved a ground for  
52 the view that perceptual experiences can be influenced by cognitive state (for references see  
53 14), consequently elaborated into the brain predictive coding approach currently dominating  
54 cognitive neuroscience (15), and positing that attention is a property of brain computation  
55 network (16). However this has been challenged by the opposite opinion that “Cognition  
56 does not affect perception” (17). Regardless whether or not such a cognitive-sensory  
57 dichotomy exists, herein we view perception and cognition as two main information streams  
58 the EF exerts its actions upon, possibly through active association.

59 We have previously described the function of two vertebrate-specific brain-expressed  
60 presynaptic gene paralogs, *NTNG1* and *NTNG2*, complementary affecting verbal  
61 comprehension and WM in human subjects, which underwent an accelerated evolution in  
62 primates and extinct hominins (1). This pair of genes is also implicated in the phenomena of  
63 antagonistic pleiotropy, a trade-off between the evolution-driven cognitive function  
64 elaboration and an array of concomitant neuropathologies, rendering the human brain  
65 phenotypically fragile (2). *Ntngs* also complementary diversify the mouse behavior (18).

66 Despite the fact that EF abrogation is a major determinant of problem behavior and  
67 disability in neuropsychiatric disorders (19), the genetics underlying EF remains elusive with  
68 no causative vector agents (e.g. genes) have yet been reported. Herein we show that *NTNG*  
69 paralogs affecting human IQ also affect mouse learning and brain executive functioning.

## 70 RESULTS

71

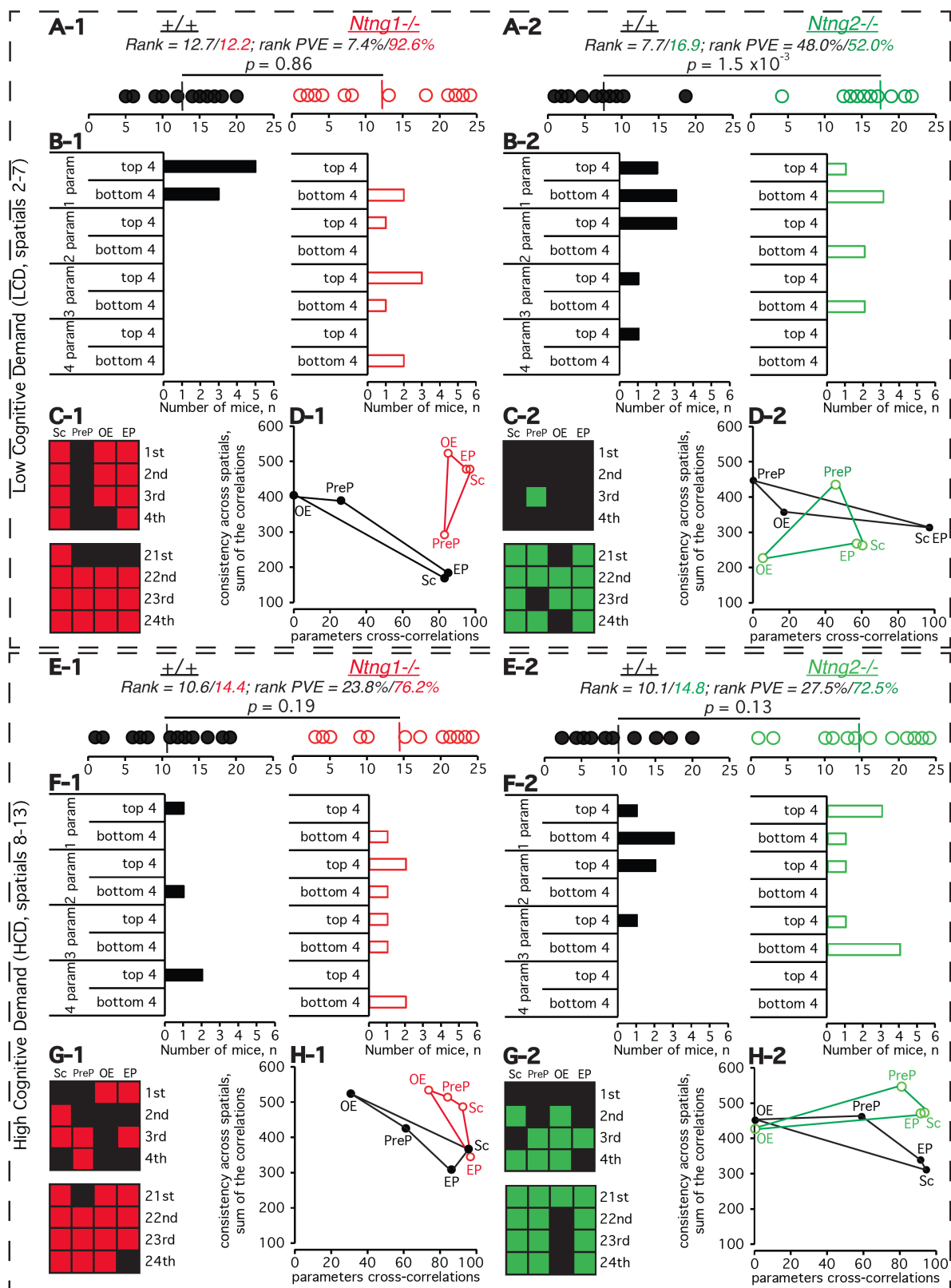
72 **Randomizing mouse genotypes to search for casual behavioral interactions.** We used a  
73 novel non-parametric data analysis approach for two distinct behavioral paradigms: 5-choice  
74 serial reaction time task (5-CSRTT, 20), and radial arm maze (RAM), measuring selective  
75 attention and impulsivity (AI), and spatial working memory (WM), respectively, in *Ntng1*<sup>-/-</sup>  
76 and *Ntng2*<sup>-/-</sup> mice. We calculated mouse genotype-independent ranking (as for a mixed  
77 population), and the rank variance (as a proportion of variance explained, PVE) for each  
78 behavioral parameter and for both paradigms. This approach allowed us to avoid common in  
79 literature a genotype-attributed single parameter reporting bias (Supplementary Figures 1  
80 (SF1) and 2 (SF2)), and permitted us to compare observed phenotypes between the both  
81 paradigms for the genetically independent groups of mice, simultaneously searching for  
82 potential interactions among them. We were able to follow the dynamics of behavioral  
83 heterogeneity and to deduce a casual inference between the mouse phenotypic and genotypic  
84 traits interaction affecting executive function (EF).

85

86 **Affected AI for both *Ntng* paralogs, and WM for the *Ntng2* gene, modulated by the**  
87 **cognitive demand.** Analysis of the 5-CSRTT data (ST1-1) has revealed that *Ntng1*<sup>-/-</sup>  
88 population of mice is characterised by an extreme span of its rank distribution (PVE>90%)  
89 occupying not only bottom 4 but also top 4 rank positions and outcompeting their wild type  
90 littermates (Fig.1(A-D)-1). *Ntng1* ablation generates mice with both strong proficit and  
91 deficit of AI, extending far beyond a single affected parameter estimate (Fig.1C,G), but with  
92 the averaged rank per a genotype undistinguishable of that of their wild type littermates, and  
93 more than 90% of variance attributable to the *Ntng1*<sup>-/-</sup> genotype (Fig.1A-1). A higher  
94 cognitive demand task phase (HCD) reduces the rank variance down to 76% but at the  
95 expense of a lower rank (Fig.1E-1), similarly to *Ntng2*<sup>-/-</sup> mice (Fig.1E-2). During the low  
96 cognitive demand task phase (LCD), contrary to *Ntng1*<sup>-/-</sup> mice, *Ntng2*<sup>-/-</sup> subjects' rank is  
97 twice lower comparing to their genetically unmodified siblings but the rank variances are the  
98 same (Fig.1(A-D)-2), and this is the main difference in the AI phenotype between the *Ntng*  
99 paralog knockouts, attributable to the magnitude of the demand.

100 Robustness of the WM deficit upon *Ntng2* deletion in mice is the most prominently  
101 evidenced by the bottom 4 mouse ranks, 13/12 out of 16 are occupied by the knockout mice  
102 (Fig.2(A-G)-2) and by low behavioral consistency across the sessions and parameters cross-  
103 correlations (Fig.2H-2) during the HCD. At the same time, the absence of *Ntng1* in mice  
104 affected only the LCD sessions performance (Fig.2(A-D)-1) but did not render them

105 behaviorally distinguishable from the wild type littermates during the HCD (Fig.2(E-H)-1).



106 Figure 1. 5-choice serial reaction time task (5-CSRTT) for *Ntn1*<sup>-/-</sup> and *Ntn2*<sup>-/-</sup> mice. See figure legend overleaf.

107

108 **Proficit and deficit in learning associated with the *Ntn*<sup>-/-</sup> genotypes.** The intricate  
109 segregation of the *Ntn*<sup>-/-</sup> gene paralogs-associated behavioral phenotypes within the distinct  
110 modules of EF (Fig.3) has prompted us to analyse the operant conditioning learning (Ln) by

111 **Figures 1,2. Attention and Impulsivity (AI) and working memory (WM) estimate and**  
112 **the effect of cognitive demand made by the analysis of rank and its variance for *Ntng1*<sup>-/-</sup>**  
113 **and *Ntng2*<sup>-/-</sup> mice. A,E.** Mice ranks and rank PVE (proportion of variance explained) based  
114 on four parameter rank measures (SF1,2) as detailed in ST1-1,2-1 (for *Ntng1*<sup>-/-</sup>) and ST1-2,2-  
115 2 (for *Ntng2*<sup>-/-</sup>). The rank sorting was done in a genotype-independent manner. Ranking for  
116 each out of four parameters was done independently of other parameters with a final re-  
117 ranking of the ranks sum to generate the final rank (shown). In case of an equal sum of the  
118 ranks, the mice were given identical ranks. PVE was calculated as a square of within  
119 genotype rank variance divided on the sum of each genotype variances squares multiplied on  
120 100%. **B,F.** Mice rank distribution across one-to-four parameters as top 4 and bottom 4  
121 performers. **C,G.** Genotype-specific rank placing among the mice. **D,H.** Behavioral  
122 consistency of mice across the sessions (*y* axis, sum of *r*<sup>2</sup> correlations of a single session  
123 ranks vs. final ranks for each mouse across the sessions) and behavioral parameter cross-  
124 correlations (*x* axis, the *r*<sup>2</sup> correlation of a parameter final ranking vs. final ranking for all 4  
125 parameters). The gene ablation-specific phenotype severity can be assessed visually by  
126 matching each parameter-corresponding vertexes of the obtained quadruples. *p* value  
127 represents a Wilcoxon rank sum test. See SM for further details.

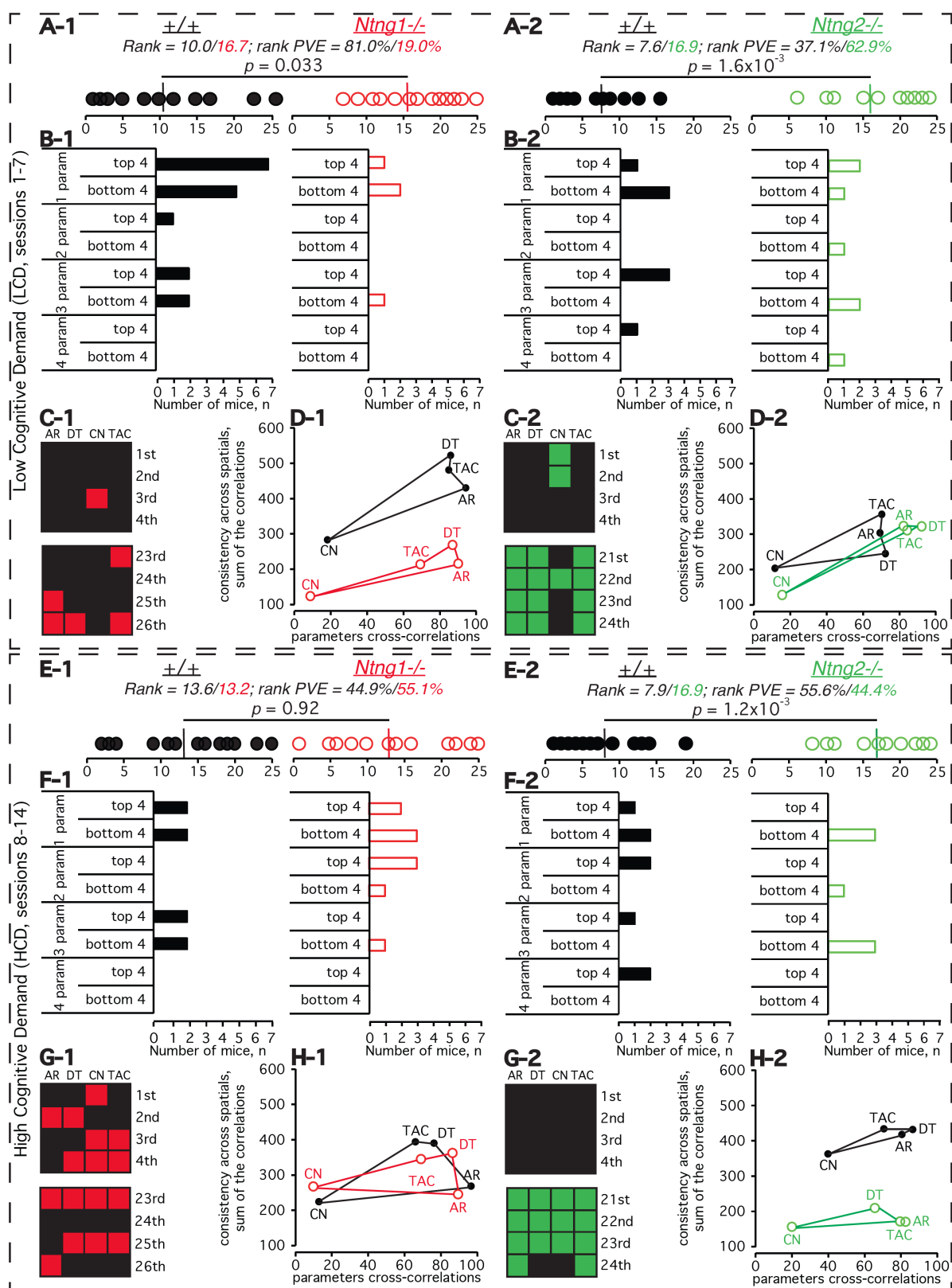
128

129 mice, assuming that AI and WM may there interact. And indeed, *Ntng1*<sup>-/-</sup> mice outperform  
130 their control group learning faster during the LCD (Fig.4(A,B)-1, LCD) but are unable to  
131 sustainably cope with the growing cognitive demand (Fig.4(A,B)-1, HCD). At the same  
132 time, *Ntng2*<sup>-/-</sup> mice display a prominent deficit of Ln (Fig.4(A,B)-2, LCD), which is  
133 becoming stronger with the growing demand to succeed (Fig.4(A,B)-2, HCD). In overall, the  
134 pattern of Ln behavior caused by the genetic ablation of both *Ntngs* completely matches that  
135 of WM testing on the RAM (Fig.2), summarised in Fig.3. The contribution of AI to the Ln  
136 deficit is further demonstrated by the rank correlations of Ln vs. AI (from Fig.1) which is  
137 stronger during the HCD for both genetically distinct mouse populations (Fig.4C-1,2).

138

139 **Complementary expression of *Ntng* paralogs in the brain and their interaction.** The  
140 robust phenotype of the abrogated EF for both *Ntng* gene paralogs affecting either AI or  
141 WM, or both, is supported by the predominant expression of both genes within the heavily  
142 loaded with the information processing brain areas, complementary sequestering them within  
143 bottom-up (for *Ntng1*) and top-down (for *Ntng2*) neuronal pathways (Fig.5A-C). The  
144 presented hierarchy for the *Ntng* paralogs brain distribution is supported by two times lower  
145 level of the *Ntng2* expression in *Ntng1*<sup>-/-</sup> background after the life-long cognitive training in

146 senile mice (Fig.5D-2), with no effect on *Ntng1* expression when *Ntng2* is absent (Fig.5D-1).



147 Figure 2. Radial arm maze (RAM) for *Ntng1*<sup>-/-</sup> and *Ntng2*<sup>-/-</sup> mice. See figure legend overleaf.

148

149 **Robust genotype prediction based on the phenotype input, the rank.** To assess the causal  
 150 inference of the genes perturbations on behavioral output we have calculated the probability  
 151 clustering for each genotype based only on the ranking data input, in genotype-blind manner

152 (Fig.6A). The obtained pattern corroborates the casual relationship between the genotypes  
153 and associated with them phenotypes of the affected EF (Fig.3) closely resembling the  
154 experimental data (Fig.1.2).

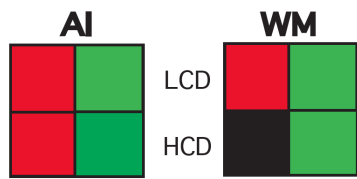


Figure 3. Summary of the EF behavioral phenotypes associated with either *Ntn1*<sup>-/-</sup> or *Ntn2*<sup>-/-</sup> gene paralogs ablation.

155

156 **Mouse behavioral phenotypic proximity assessment.** To calculate a phenotypic distance  
157 between the genotypes comprising a single mixed population we used the obtained ranks and  
158 plotted them against the related PVE for each behavioral parameter, generating two linear  
159 plots (Fig.6B), each representing a single contributing genotype. This let us further to  
160 calculate the phenotypic distance (using the classical Euclidean geometry) between the  
161 genotypes as the shortest distance between two parallel lines. The obtained geometrical plots  
162 are in a full agreement with the experimentally observed behaviors (Figs.1-3) but  
163 additionally pinpoint the contribution of each individual parameter sometimes located outside  
164 of the main cluster with others, e.g. PreP for the *Ntn1*<sup>-/-</sup> (Fig.6B-1, AI-LCD), OE for the  
165 *Ntn1*<sup>-/-</sup> (Fig.6B-2, AI-HCD), and CN for the *Ntn2*<sup>-/-</sup> (Fig.6B-2, WM-LCD). Using the Ln  
166 rank and its PVE from Fig.4 as (x,y) coordinates we have assessed the phenotypic proximity  
167 of the *Ntn1*<sup>-/-</sup> and *Ntn2*<sup>-/-</sup> mouse AI and WM phenotypes to the Ln deficit.

168

169 **Task learning (Ln) as an outcome of AI and MW interactions.** With the assumption that  
170 shorter distance from the Ln coordinates to the genotype-specific linear plot generates higher  
171 likelihood that the given genotype contributes to the Ln associated behavior, we were able to  
172 build a relationship graph among the Ln, AI and WM interactions modulated by the  
173 cognitive demand (Fig.7A). The dynamics of the *Ntn* gene paralogs hierarchy interaction is  
174 presented on Fig.7B, calculated by the reciprocal plug-in of the rank and its PVE for one  
175 gene paralog into the linear plot for the other one (ST7).

176

177 DISCUSSION

178

179 **Inferring casual relationship for the *Ntn* paralogs ablation caused perturbations with  
180 the EF abrogation phenotypes.** The hierarchy of WM and selective attention interplay has  
181 been always a point of fierce debate (21). In the present study we look at this interaction  
182 through the prism of mouse operant conditioning learning ability, perturbed by either of

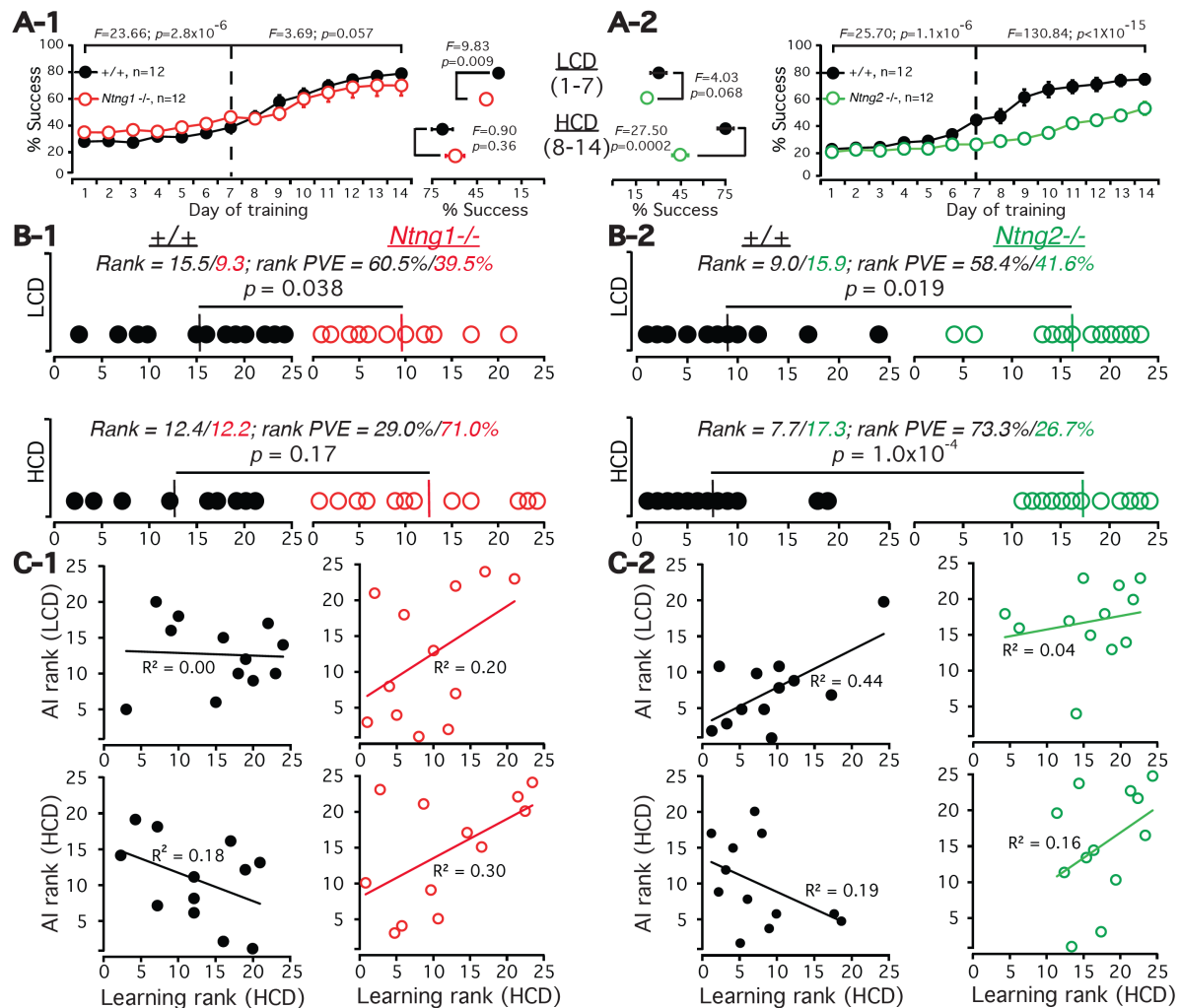


**Figure 4. Operant conditioning (5-CSRTT) Learning (Ln) by *Ntn1*<sup>-/-</sup> and *Ntn2*<sup>-/-</sup> mice.** A. Learning curves for the operant conditioning learning (reward collection) over the training period (spatial 1 of 5-CSRTT) with averaged performance behavior for the days (1-7) and (8-14), middle panel, defined as low cognitive demand (LCD) and high cognitive demand (HCD) sessions, respectively. One and two-way ANOVA was used for the statistics. B. Ranks and PVE comparisons over the LCD and HCD. The rank sorting was done in a genotype-independent manner, similar to Fig.1 and Fig.2, but using only one parameter, success (Sc), see ST4-1 and ST4-2. Rank statistics was by Wilcoxon rank sum test. C. Learning (Ln) vs. attention and impulsivity (AI) rank correlations (from Fig.1A-1,2).

183

184

185 *Ntn* gene paralogs ablation (Fig.4). Since it is known that averaging animal behavior across  
 186 individual subjects (SF1-1,1-2) may smear out control variables (22), we used rank instead  
 187 of classical data mean (Figs.1-3) approach and the rank variance (proportion of variance  
 188 explained, PVE) per genotype, as a measure of difference (23:p.16), to assess the behavioral  
 189 variability caused by the genetic variations interacting with the experimental demand. To  
 190 proof casual inferences between the behavior of *Ntn*<sup>-/-</sup> mice and the gene ablation, we used  
 191 mouse rank as a randomized dependent variable of the mixed population noting that any  
 192 other non-randomized variables would be only correlational (24). That is, we have presented  
 193 the mouse behavioral rank distribution as a function of genotype, when one of the *Ntn*

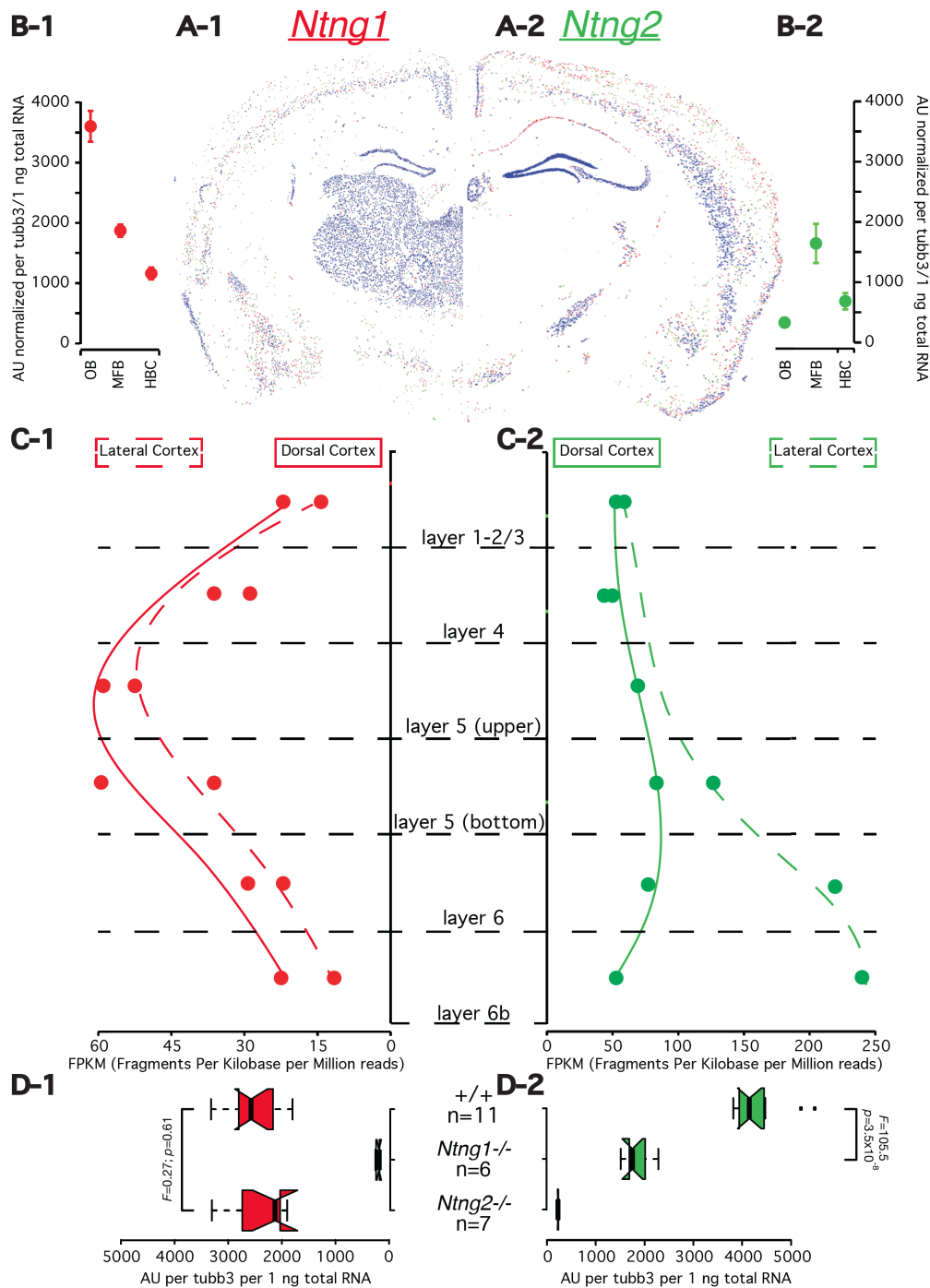


**Figure 5. Complementary expression and transcription of *Ntn1* and *Ntn2* paralogs in the mouse brain.** (A) *In situ* hybridization of *Ntn1* (left) and *Ntn2* (right) in the mouse brain. From Allen Brain Atlas, accession numbers are RP\_050607\_01\_H05 and RP\_050810\_04\_D08, respectively. The expression colors are inverted. (B) qRT-PCR of total mRNA for *Ntn1* and *Ntn2* paralogs in rough brain fractions of adult naïve male mice (7-8 months old): OB = olfactory bulb; MFB = mid- and front brain; HBC = hindbrain and cerebellum, n=6 mice (ST5-1). (C) Total level of *Ntn1* and *Ntn2* mRNA expression calculated based on RNA-seq of the mouse brain cortical layers reconstructed for *Ntn1* and *Ntn2* paralogs expression from GSE27243 generated by Belgard et al. (51). See Supplementary Methods (SM) for the details of data processing, ST5-2, ST5-2\_Cuff and ST5-2\_iReck (zipped) for the transcriptome assembly. (D) Effect of genetic background on *Ntn1* and *Ntn2* paralogs expression level in MFB as detected by qRT-PCR (ST5-3). Senile (20-21 months old) life-long cognitively trained mice have been used (from Fig.1). One-way ANOVA was used for the statistics.

194

195

196

197

paralogs has been genetically ablated. At the same time, we have tried to elaborate on the statement that the structure of genotype–phenotype map is the matter and not the variance components of the population itself (25). The open question in such genotype-phenotype

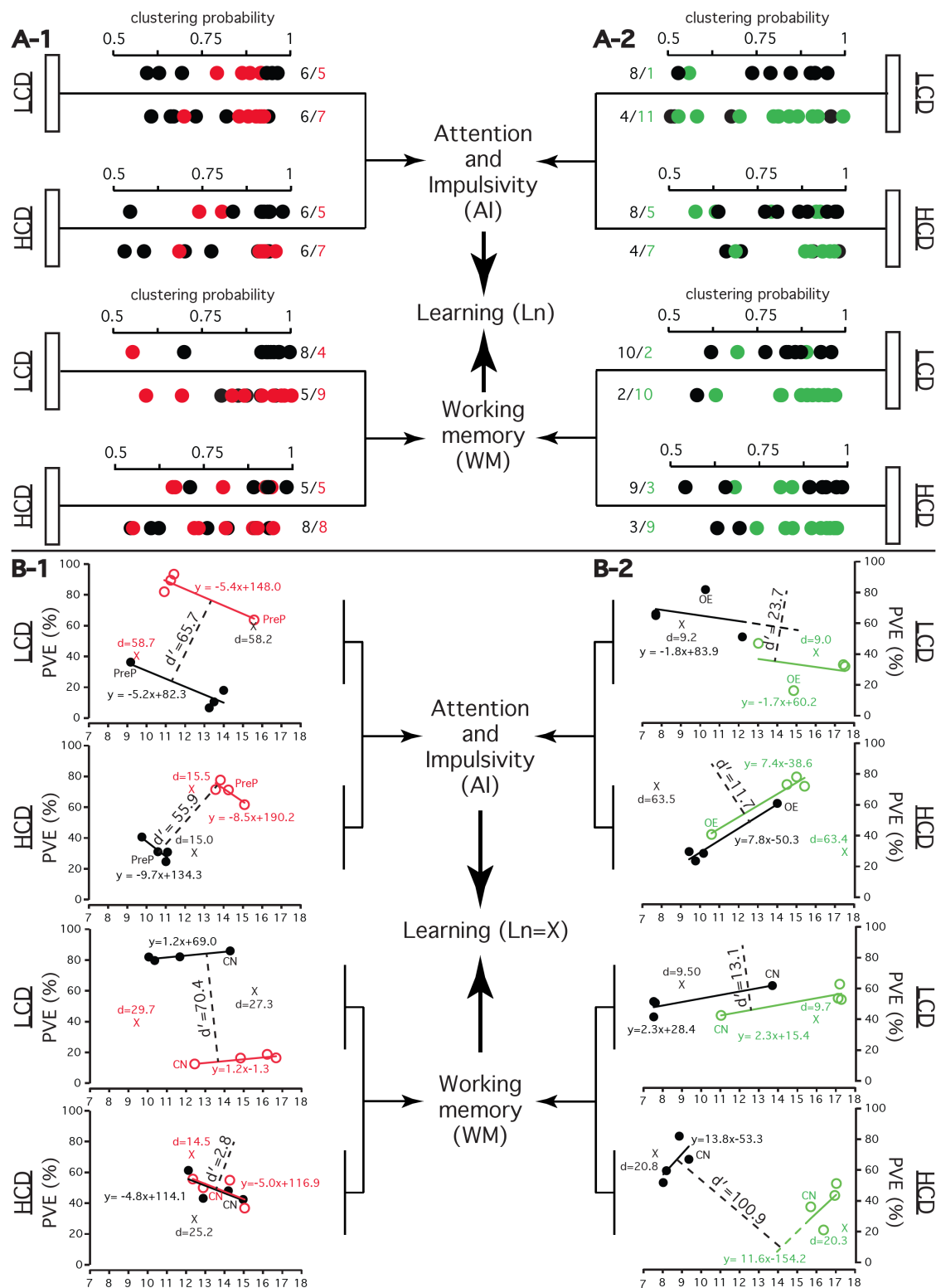


**Figure 6.** Behavioral phenotypic proximity assessment for the *Ntn1*<sup>-/-</sup> and *Ntn2*<sup>-/-</sup> genotypes and their wild type littermates by two approaches: genotype predictions by C-means fuzzy clustering (A), and by linear regression plot of genotype-specific rank PVE vs. rank (B). **A.** Casual genotype-phenotype relationship evidence. C-means fuzzy clustering (Euclidean C-means) was done in a genotype-blind manner as described in SM. See ST6-1 and ST6-2 for the exact values of clustering probabilities. **B.** Descriptive proximity of the operant conditioning learning explained by the AI and WM phenotypes for *Ntn1*<sup>-/-</sup> paralog mice. Distance between the genotypes ( $d'$ , dashed line), presented geometrically by the linear equation, was calculated as  $d' = |c_2 - c_1|$ , where  $ax + by + c = 0$  (Euclidean geometry). Distance from the learning coordinates ( $L_n$ ) to the genotype-describing line was calculated as  $d = |c - (y_{L_n} - ax_{L_n})|$ . Rank ( $x$  coordinates) and PVE values ( $y$  coordinates) are from Fig. 1A,E (AI); Fig. 2A,E (WM); and Fig. 4B ( $L_n$ ), ST7. Data for the *Ntn1*<sup>-/-</sup>/wt population (RAM) are likely to incorporate 7.69% error since they were not normalised to the total number of animals as for the other populations ( $n = 26$  vs.  $n = 24$  mice).

199 interaction paradigm is to what degree a genetic variability is capacitive enough to explain  
200 the phenotypic variance and the strength of such casual interaction. More specifically, how  
201 far the behavioral (whole organism) variability (under the pressure of the growing cognitive  
202 demand) represents the neuronal (cellular) variability caused by a gene knockout exerted  
203 perturbations.

204

205 **Cognitive phenotypes of the *Ntn1*<sup>-/-</sup> mice.** None of the vertebrate brain specific  
206 presynaptically expressed *Ntn1*<sup>-/-</sup> nor *Ntn2*<sup>-/-</sup> mice exhibit gross anatomical or  
207 developmental abnormalities (26) rendering them unique models to study the brain cognitive  
208 functions in the absence of any “house-keeping” functional distortions and avoiding gene-  
209 manipulations-exerted non-casual confounders. Noteworthy the resemblance of *Ntn1*<sup>-/-</sup> and  
210 *Ntn2*<sup>-/-</sup> mice behavioral phenotypes with the human schizophrenia subjects behavioral  
211 etiology (characterised by the EF control pathologies), both genes have been reportedly  
212 associated with (1,2). Two different populations of mice were used for two different  
213 behavioral paradigms to avoid the phenomena of learning transfer between the behavioral  
214 tests, and, at the same time, to check for the genotype induced phenotypic stability across the  
215 different paradigms but sharing the principal underlying component of WM testing. And  
216 indeed, slow operant conditioning learning (5-CSRTT) for *Ntn2*<sup>-/-</sup> mice has been recorded  
217 (Fig.4A,B-2) and is explainable by the dysfunction of procedural (working) memory robustly  
218 affecting the RAM performance (Fig.2A-H-2).

219

220 **Behavior consistency assessment using rank.** We have also characterised the behavior of  
221 mice as a heterogeneously randomized population through the assessment of rank  
222 consistency across the sessions and relative to other parameters (Figs.1-2D,H). Parameters  
223 cross-correlation coefficients ( $r^2$ , x axis) indicate a probability value of how much the rank  
224 of a mouse for a certain parameter contributes to the global (total) ranking comprised of all  
225 four parameters. If a mouse fails to keep its performance consistent either over the multiple  
226 sessions or a parameter, its rank is instantly occupied either by the same or by a different  
227 genotype littermate, and such event would be dynamically reflected in the  $r^2$ . But ranks  
228 changes and their permutations may not necessary have any dramatic consequences in the  
229 total rank calculations as soon the rank fluctuations are taking place within the same  
230 genotype-specific variance boundaries. But they are more reflective of a behavior  
231 inconsistency of an individual mouse reflected in the sum of the correlation variances per  
232 spatial or session (y axis).

233

234 **WM deficit driven optimal strategy deprivation for the *Ntng2*<sup>-/-</sup> mice.** The global spatial  
 235 WM deficit for the *Ntng2*<sup>-/-</sup> mice has been found robustly expressed across the three RAM  
 236 parameters (Fig.2A-H-2) except for CN (arm choice number during the first 8 arm entries).  
 237 This parameter represents a strategy development (during LCD) and its optimisation (during  
 238 HCD) for the maximum reward collection efficiency, akin predictive type behavior of the  
 239 likelihood of potential success. The fact that the *Ntng2*<sup>-/-</sup> mice outperform their wt littermates  
 240 in CN (but during the LCD only, Fig.2C-2) reflects the chosen strategy (or a complete lack  
 241 of any) of a pure random choice of a baited arm to visit, corroborating the global WM deficit  
 242 (inability for strategic thinking) for the knockouts (evident from the other parameters) but  
 243 with an opposite valence.

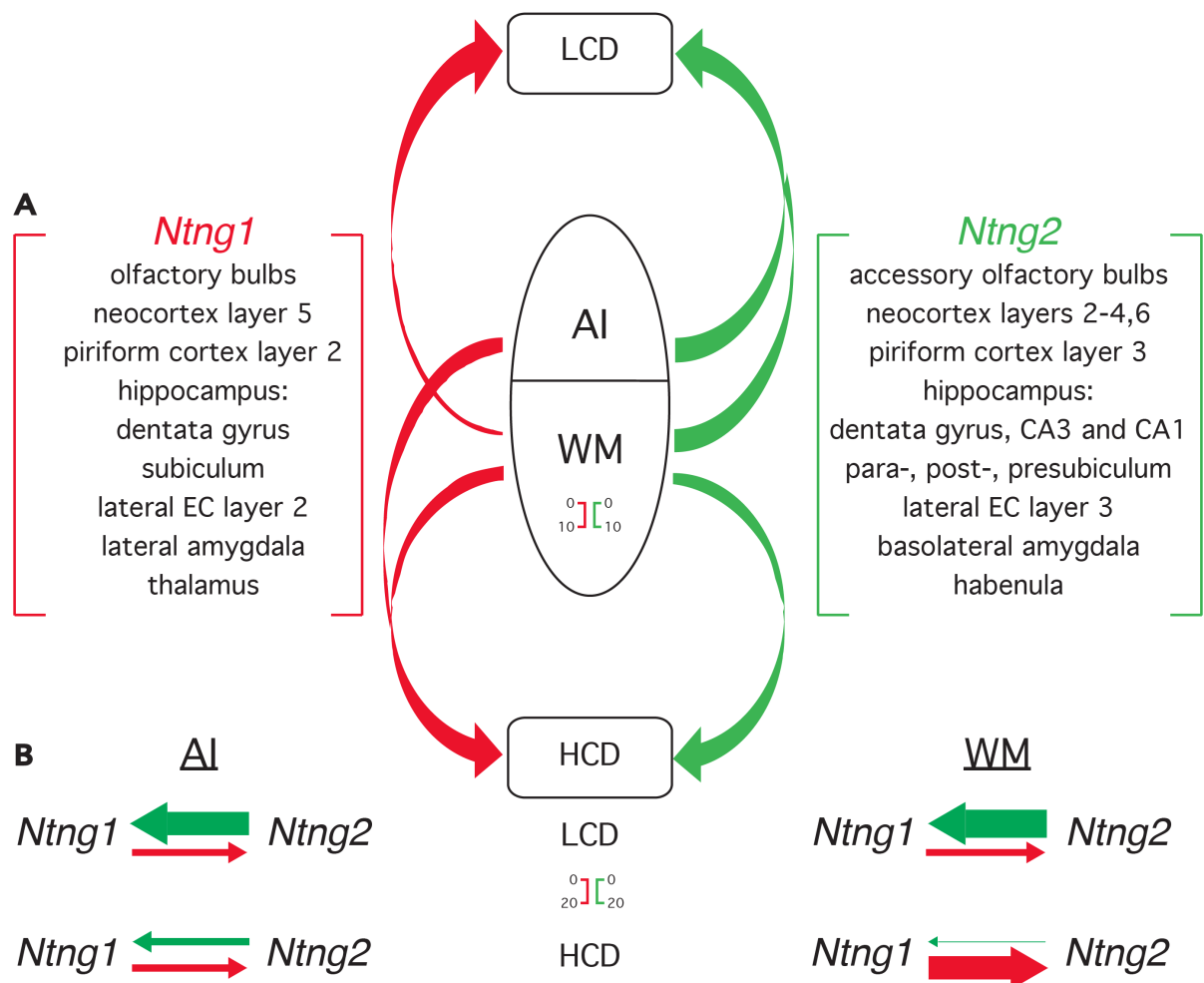


Figure 7. *Ntng* paralogs interaction as a molecular correlate of AI and WM modalities during learning. A. AI and WM interactions modulated by the cognitive demand during the operant conditioning earning (Ln), complementary contributed by the differentially expressed *Ntng* paralogs (see Fig.5 and (52)). B. Dynamicity of *Ntng* paralogs hierarchy interactions under LCD and HCD contributing to AI and WM. Each arrow base width (the scale bar is shown) is expressed in AU and corresponds to  $(1/d*100)$  value from Fig.6B (for Ln=X), see ST7. Out of scale arrows (AI-*Ntng1*-LCD and AI-*Ntng2*-HCD) are not shown.

244

245

246 **Paralogs brain expression supporting the behavioral phenotypes.** The phenotypic

247 complementarities among the *Ntng1*<sup>-/-</sup> and *Ntng2*<sup>-/-</sup> mice, associated either with the abrogated  
248 AI or WM, or both (Fig.3), are supported by the complementary brain expression pattern of  
249 these gene paralogs (Fig.5A). If *Ntng1* is expressed mostly in the primary somatosensory  
250 gating areas (e.g. OB, thalamus and hypothalamus nuclei, midbrain and medulla, Fig.5A,B-  
251 1), *Ntng2* dominates within the cortex (with the skewed expression saturation towards the  
252 lateral cortex), hippocampus (HPC), amygdala and claustrum, endopiriform and reticular  
253 nuclei, Fig5A-2), pointing the gene role of parsing top-down signals. If the sensory  
254 perception, as an entry point into the attentional state, is determined by the strength of the  
255 subcortical thalamus-PFC (pre-frontal cortex) pathways (27), the reciprocal interactions  
256 between mPFC and HPC are pivotal for the WM functioning (28,29), with the HPC known  
257 to encode perceptual representations into memories through the correct attentional states  
258 (30). Complementing this, thalamocortical projections are vital for mediating sensation,  
259 perception, and consciousness (31-33). It is assumed that WM, despite its distributed nature  
260 (34), consists of an executive component spread over the frontal lobes and sensory cortices  
261 and interacted by the attention (7,35).

262

### 263 **Brain lamina-specific enrichment and EF control contribution by the *Ntng* paralogs.**

264 The emergence of a six-layered neocortex is a known hallmark of the mammalian brain  
265 specialization devoted to the EF control (36,37). Both *Ntng* gene paralogs are extensively  
266 expressed and mutually sequestered among the separate layers of the cortex (Fig.5C). *Ntng1*  
267 is predominantly located in layers 4/5 (Fig.5C-1), probably supporting the arrival of the  
268 bottom-up signals (38), while *Ntng2* is located in the superficial layers 2/3 and deeper layers  
269 5/6 (Fig.5C-2), reported as a source of top-down inputs in attention and WM demanding  
270 tasks (39). Besides that, *Ntng2* has been also marked as a gene classifier for the granule  
271 neurons enriched in the cortex layer 6 (40). In overall, the complementary patterning of the  
272 *Ntng* gene paralogs expression supports the laminar-specific distribution of the attention-  
273 directed modalities.

274

275 **Evidence for the cognitive control taking over the perceptual load.** Analysing AI and  
276 WM interaction during the task learning (Fig.7A), we have revealed that HCD recruits more  
277 *Ntng1* (bottom-up) expressing circuitry comparing to LCD, both by WM and AI, reciprocally  
278 replacing the preceding *Ntng2* (top-down) contribution. This potentially points to an  
279 augmented peripheral sensory control by upregulating the bottom-up information stream.  
280 How to explain such intricacy? Attention exploits a conserved circuitry motif predating the  
281 neocortex emergence (41) and WM probably exapts the motor control of forward action

282 modeling also elaborated since ancient times (42). The archaic origin of both modalities  
283 limits the fundamental brain resource and constrains information processing, forcing trade-  
284 offs among the objects of targeted attention through the top-down control and, possibly,  
285 causing a competition between the sensory inputs (43,44) by driving attention at  
286 representations in sensory areas where the latter gains entry into WM (7). A model has been  
287 proposed that selective attention control is directly linked to the executive control part of the  
288 WM system (45) corroborating the statement that attention and WM should no longer be  
289 regarded as two separate concepts, see (46) for references. The top-down control of primary  
290 sensory processing by higher cortical areas (through the recurrent inputs) has an essential  
291 role in sensory perception, as we have just demonstrated. The pervasive penetration of the  
292 cognitive control, supported by *Ntng2*, affects the sensory inputs, provided by the *Ntng1*  
293 expression.

294

295 **An IQ for mice.** The EF control variance attributes to the cognitive performance variance  
296 and does not exist independently of general intelligence (47) as a critical determinant of  
297 human cognition (48). It is no wonder then that, in our hands, the genes affecting WM and  
298 attention in mice are the same ones affecting IQ in humans (1) and also associated with a  
299 variety of devastating neurological disorders (2) representing a strong case of antagonistic  
300 functional pleiotropy. The open challenge is to find out to what degree, using *Ntng* gene  
301 paralogs as benchmarks, we would be able to conclusively draw on either domain specific or  
302 domain general cognitive abilities of mice, or any other non-human animal subjects  
303 behavioral intelligence.

304

305 Conclusively, *Ntng1* participates in bottom-up, and *Ntng2* in top-down brain  
306 information flows support, representing an integrative complementary agreement between  
307 perception and cognition as two interacting functions of the brain.

308

309 CONCLUSION

310

311 The view of Brain (and Mind) as a modular (domain) system is appealing to evolutionary  
312 thinking (49) but is strongly biased towards “the prominence of neural reductionism” (22)  
313 dominating the modern neuroscience. There is no strict definition of what a cognitive domain  
314 is but it can be viewed as a product of interaction between the top-down and bottom-up  
315 underlying neuronal circuits forming bidirectional feedback loops for the executively  
316 decisive and sensory information flows controlling its own self. Genes selectively expressed

317 within such circuits via a non-overlapping pattern represent a tantalizing target to study the  
318 cognitive domain make-up and its evolution. An ancient *Ntng* gene duplication (>500 million  
319 years ago, preceding the Cambrian explosion) and subsequent co-evolution within the  
320 vertebrate genomes made *Ntng* gene paralogs to segregate within the top-down and bottom-  
321 up evolving information paths, presumably via subfunctionalisation, under the growing  
322 ecological demand (first land/water fish met) but different epistatic environment, both gene  
323 paralogs are embedded into. Perception and cognition interplay had eventually culminated  
324 in a reflectively subjective representation of the external world, also called consciousness,  
325 and explicitly controlled by the EF. Unrevealing molecular correlates of the domain-specific  
326 cognitive abilities would help us better understand behavior, e.g. to clearly dissect it on  
327 actions (as self-generated thoughts) and responses (cue-induced actions), as a decomposable  
328 conjunction supporting the robust functioning of the Brain holistic state.

329

## 330 MATERIALS AND METHODS

331

332 **Animals and behavioral set-ups.** The original behavioral datasets have been partially  
333 published by us in (18). All raw data are provided in [ST1-ST4](#) and [SF1,2](#). Knockout animals  
334 and the behavioral set-ups are described in (18).

335

336 **Data analysis.** All raw data including their ranks and PVE calculations with all formulas and  
337 graphs are presented in [ST1-ST4](#). The dynamics of the rank change for a specific parameter  
338 over the course of study and its congruence with other parameters is depicted on [Figs.1-](#)  
339 [2D,H](#). No robustness calculations of the rank distribution pattern resistance to a sequential  
340 removal of a single behavioral subject were done; neither estimate for the minimal number of  
341 the top/bottom ranks representing the obtained pattern, it was empirically decided to be equal  
342 to top and bottom four ([Figs.1-2](#)).

343

344 **Definition of LCD and HCD.** During the 5-CSRTT the cognitive demand was incremented  
345 by a shorter cue duration and longer inter-trial intervals, as specified in (18). As for the  
346 RAM, the second week of testing (sessions 8-14) was done with half-closed/half-opened  
347 doors under the gradually building cognitive demand, internally driven by the behavior  
348 optimisation strategy for the maximum likelihood of reward collection, top-down executive-  
349 attentional pressure to optimise the behavioral performance outcome, contextually similar to  
350 the operant conditioning learning (Ln) of spatial 1 of the 5-CSRTT ([Fig.4](#)).

351

352 **Real-time qPCR (qRT-PCR).** Primers specifically targeting beginning of each *Ntng* gene  
353 paralogs full-length transcripts were designed using Primer3Plus:  
354 <http://www.bioinformatics.nl/cgi-bin/primer3plus/primer3plus.cgi>. Frozen brains RNA was  
355 isolated from the MFB using RNeasy Plus Minikit (Qiagen) and the cDNA was synthesised  
356 by the QuantiTect<sup>®</sup> Reverse Transcription kit (Qiagen) using a mix of the random hexamers  
357 and oligodT primers. cDNA synthesised from 1 ng of total RNA was used per a single qRT-  
358 PCR reaction. The lack of genomic DNA and the absence of external contamination were  
359 confirmed by the RT-minus reactions. Neuronal-specific *tubb3* transcript ( $\beta$ -tubulinIII) was  
360 used as an internal normaliser during the qRT-PCR co-amplifications. The  $C_t$  values were  
361 collected at the threshold value of 0.4 and the arbitrary units (AU) were calculated as:

$$362 \quad 2^{-(C_t(\text{amplicon}) - C_t(\text{normalizer}))} * 10,000$$

363

364 **RNA-seq cortical layers *Ntng* transcriptome reconstruction.** See [SM](#) for the details.

365

366 **Fuzzy C-Means Clustering.** Represents a type of a sequential competitive learning  
367 algorithm exhibiting the stochastic approximation problem (50). Was used for the genotype  
368 predictions based on the behavioral ranks input under the genotype-blind input conditions.  
369 The details are described in the [SM](#).

370

371 **Statistics.** Correlation coefficients ( $r^2$ ) were obtained with Excel. One and two-way  
372 ANOVA was calculated using StatPlus (AnalystSoft Inc.). Wilcoxon rank sum test was done  
373 by Matlab (v.7.9.0 2009b) by the function *ranksum*.

374

375 SUPPLEMENTARY MATERIALS ([SM](#))

376 Contain Supplementary Figures ([SF1-2](#)), Tables ([ST1-7](#)), Methods and References. [ST1-ST5](#)  
377 are provided as Excel files.

378

379 ACKNOWLEDGEMENTS

380 This work was in part supported by the “Funding Program for World-Leading Innovative  
381 R&D on Science and Technology (FIRST Program)” initiated by the Council for Science  
382 and Technology Policy (CSTP), and KAKENHI 15H04290 from the Japan Society for the  
383 Promotion of Science (JSPS).

384

385 COMPETING INTERESTS

386 Authors would like to express a lack of any competing interests associated with the work.

387 REFERENCES

388

- 389 1. Prosselkov P, Hashimoto R, Polygalov D, Ohi K, Zhang Q, McHugh JT, Takeda M, and  
390 Itohara, S. (2016) Cognitive endophenotypes of modern and extinct hominins associated  
391 with *NTNG* gene paralogs. *Biomedical Genetics and Genomics*, **1**(1): 5–13.  
392 <http://doi.org/10.15761/BGG.1000103>
- 393 2. Prosselkov P, Polygalov D, Zhang Q, McHugh JT and Itohara S. (2016) Cognitive domains  
394 function complementation by *NTNG* gene paralogs. *Biomedical Genetics and Genomics*,  
395 **1**(1): 24–33. <http://doi.org/10.15761/BGG.1000105>
- 396 3. Mar AC, Horner AE, Nilsson SRO, Alsio J, Kent BA, Kim CH, Holmes A, Saksida LM,  
397 Bussey TJ. (2013) The touchscreen operant platform for assessing executive function in  
398 rats and mice. *Nature Protocols*, **8**(10): 1985–2005. <http://doi.org/10.1038/nprot.2013.123>
- 399 4. Mandelman SD and Grigorenko EI (2011) "Intelligence". In *The Cambridge Handbook of*  
400 *Intelligence*. Edited by Sternberg RJ and Kaufmann SB. Cambridge University Press.  
401 ISBN: 052173911X.
- 402 5. Matzel LD and Kolata S. (2010) Selective attention, working memory, and animal  
403 intelligence. *Neuroscience and Biobehavioral Reviews*, **34**(1): 23–30.  
404 <http://doi.org/10.1016/j.neubiorev.2009.07.002>
- 405 6. Baddeley A. (1992) Working Memory. *Science*, **255**(5044): 556–559.  
406 <http://doi.org/10.1126/science.1736359>
- 407 7. Carruthers P. (2013) Evolution of working memory. *Proceedings of the National Academy*  
408 *of Sciences of the United States of America*, **110**(S2): 10371–10378.  
409 <http://doi.org/10.1073/pnas.1301195110>
- 410 8. Trubutschek D, Marti S, Ojeda A, King J-R, Mi Y, Tsodyks M and Dehaene S. (2016) A  
411 theory of working memory without consciousness or sustained activity. *bioRxiv*.  
412 <http://doi.org/https://doi.org/10.1101/093815>
- 413 9. Soto D and Silvanto J. (2014) Reappraising the relationship between working memory and  
414 conscious awareness. *Trends in Cognitive Sciences*, **18**(10): 520–525.  
415 <http://doi.org/http://dx.doi.org/10.1016/j.tics.2014.06.005>
- 416 10. Leong YC, Radulescu A, Daniel R, DeWoskin V and Niv Y. (2017) Dynamic Interaction  
417 between Reinforcement Learning and Attention in Multidimensional Environments.  
418 *Neuron*, **93**(2): 451–463. <http://doi.org/10.1016/j.neuron.2016.12.040>
- 419 11. Cahen A and Tacca MC. (2013) Linking perception and cognition. *Frontiers in*  
420 *Psychology*, **4**: e144. <http://doi.org/10.3389/fpsyg.2013.00144>

- 421 12. Potter MC. (2012) Conceptual Short Term Memory in Perception and Thought. *Frontiers*  
422 *in Psychology*, **3**: e113. <http://doi.org/10.3389/fpsyg.2012.00113>
- 423 13. Brown H, Friston K and Bestmann S. (2011) Active Inference, Attention, and Motor  
424 Preparation. *Frontiers in Psychology*, **2**: e218. <http://doi.org/10.3389/fpsyg.2011.00218>
- 425 14. Mroczko-Wąsowicz A. (2016) Editorial: Perception-Cognition Interface and Cross-Modal  
426 Experiences: Insights into Unified Consciousness. *Frontiers in Psychology*, **7**: e1593.  
427 <http://doi.org/10.3389/fpsyg.2016.01593>
- 428 15. Clark A. (2013) Whatever next? Predictive brains, situated agents, and the future of  
429 cognitive science. *Behavioral and Brain Sciences*, **36**(3): 181–204.  
430 <http://doi.org/10.1017/s0140525x12000477>
- 431 16. Rosenberg MD, Finn ES, Scheinost D, Constable RT and Chun MM. (2017)  
432 Characterizing Attention with Predictive Network Models. *Trends in Cognitive Sciences*,  
433 **21**(4): 290–302. <http://doi.org/10.1016/j.tics.2017.01.011>
- 434 17. Firestone C and Scholl CF. (2015) Cognition does not affect perception: Evaluating the  
435 evidence for “top-down” effects. *Behavioral and Brain Sciences*, **39**: e229.  
436 <http://doi.org/https://doi.org/10.1017/S0140525X15000965>
- 437 18. Zhang Q, Goto H, Akiyoshi-Nishimura S, Prosselkov P, Sano C, Matsukawa H, Yaguchi  
438 K, Nakashiba T and Itohara S. (2016) Diversification of behavior and postsynaptic  
439 properties by netrin-G presynaptic adhesion family proteins. *Molecular Brain*, **9**(1): e6.  
440 <http://doi.org/10.1186/s13041-016-0187-5>
- 441 19. Royall DR, Lauterbach EC, Cummings JL, Reeve A, Rummans TA, Kaufer DI, LaFrance  
442 CW, Coffey CE. (2002) Executive Control Function: A Review of Its Promise and  
443 Challenges for Clinical Research. *The Journal of Neuropsychiatry and Clinical*  
444 *Neurosciences*, **14**(4): 377–405. <http://doi.org/10.1176/jnp.14.4.377>
- 445 20. Bari A, Dalley JW and Robbins TW (2008) The application of the 5-choice serial reaction  
446 time task for the assessment of visual attentional processes and impulse control in rats.  
447 *Nature Protocols*, **3**(5), 759–767. <http://doi.org/10.1038/nprot.2008.41>
- 448 21. Abrahamse E, Majerus S, Fias W and Dijck J-P. (2015) Editorial: Turning the Mind’s Eye  
449 Inward: The Interplay Between Selective Attention and Working Memory. *Frontiers in*  
450 *Human Neuroscience*, **9**: (e616). <http://doi.org/10.3389/fnhum.2015.00616>
- 451 22. Gomez-Marin A and Mainen ZF. (2016) Expanding perspectives on cognition in humans,  
452 animals, and machines. *Current Opinion in Neurobiology*, **37**: 85–91.  
453 <http://doi.org/10.1016/j.conb.2016.01.011>

- 454 23. Laudański LM. (2013) Between Certainty and Uncertainty: Statistics and Probability in  
455 Five Units with Notes on Historical Origins and Illustrative Numerical Examples  
456 (Intelligent Systems Reference Library) Springer. ISBN-13: 978-3642256967.
- 457 24. Jazayeri M and Afraz A (2017) Navigating the Neural Space in Search of the Neural Code.  
458 *Neuron*, **93**(5), 1003–1014. <http://doi.org/10.1016/j.neuron.2017.02.019>
- 459 25. Paixão T and Barton NH. (2016) The effect of gene interactions on the long-term response  
460 to selection. *Proceedings of the National Academy of Sciences*, **113**(16): 4422–4427.  
461 <http://doi.org/10.1073/pnas.1518830113>
- 462 26. Nishimura-Akiyoshi S, Niimi K, Nakashiba T and Itohara S. (2007) Axonal netrin-Gs  
463 transneuronally determine lamina-specific subdendritic segments. *Proceedings of the*  
464 *National Academy of Sciences of the United States of America*, **104**(37): 14801–14806.  
465 <http://doi.org/10.1073/pnas.0706919104>
- 466 27. Wimmer RD, Schmitt LI, Davidson TJ, Nakajima M, Deisseroth K, Halassa MM. (2015)  
467 Thalamic control of sensory selection in divided attention. *Nature*, **526**(7575): 705–709.  
468 <http://doi.org/10.1038/nature15398>
- 469 28. Jin J and Maren S. (2015) Prefrontal-Hippocampal Interactions in Memory and Emotion.  
470 *Frontiers in Systems Neuroscience*, **9**: e170. <http://doi.org/10.3389/fnsys.2015.00170>
- 471 29. Spellman T, Rigotti M, Ahmari SE, Fusi S, Gogos JA, Gordon JA. (2015) Hippocampal–  
472 prefrontal input supports spatial encoding in working memory. *Nature*, **522**(7556): 309–  
473 314. <http://doi.org/10.1038/nature14445>
- 474 30. Aly M and Turk-Browne NB (2016) Attention promotes episodic encoding by stabilizing  
475 hippocampal representations. *Proceedings of the National Academy of Sciences of the*  
476 *United States of America*, **113**(4): E420–429. <http://doi.org/10.1073/pnas.1518931113>
- 477 31. Riga D, Matos MR, Glas A, Smit AB, Spijker S and Oever MCV. (2014) Optogenetic  
478 dissection of medial prefrontal cortex circuitry. *Frontiers in Systems Neuroscience*, **8**:  
479 E230. <http://doi.org/10.3389/fnsys.2014.00230>
- 480 32. John ER. (2002) The neurophysics of consciousness. *Brain Research Reviews*, **39**(1): 1–  
481 28. [http://dx.doi.org/10.1016/S0165-0173\(02\)00142-X](http://dx.doi.org/10.1016/S0165-0173(02)00142-X)
- 482 33. Alitto HJ and Usrey WM. (2003) Corticothalamic feedback and sensory processing.  
483 *Current Opinion in Neurobiol.*, **13**(4): 440–445. [http://10.1016/S0959-4388\(03\)00096-5](http://10.1016/S0959-4388(03)00096-5)
- 484 34. Christophel TB, Klink PC, Spitzer B, Roelfsema PR and Haynes J-D. (2017) The  
485 Distributed Nature of Working Memory. *Trends in Cognitive Sciences*, **21**(2): 111–124.  
486 <http://doi.org/10.1016/j.tics.2016.12.007>
- 487 35. Postle BR. (2006) Working memory as an emergent property of the mind and brain.  
488 *Neuroscience*, **139**(1): 23–38. <http://doi.org/10.1016/j.neuroscience.2005.06.005>

- 489 36. Smaers JB, Gómez-Robles A, Parks AN and Sherwood CC. (2017) Exceptional  
490 Evolutionary Expansion of Prefrontal Cortex in Great Apes and Humans. *Current*  
491 *Biology*, **27**(5): 714-720. <http://doi.org/10.1016/j.cub.2017.01.020>
- 492 37. Hardung S, Epple R, Jäckel Z, Eriksson D, Uran C, Senn V, Gibor L, Yiezhari O, Diester  
493 I. (2017) A Functional Gradient in the Rodent Prefrontal Cortex Supports Behavioral  
494 Inhibition. *Current Biology*, **27**(4): 549–555. <http://doi.org/10.1016/j.cub.2016.12.052>
- 495 38. Nandy AS, Nassi JJ and Reynolds JH. (2017) Laminar Organization of Attentional  
496 Modulation in Macaque Visual Area V4. *Neuron*, **93**(1): 235–246.  
497 <http://doi.org/10.1016/j.neuron.2016.11.029>
- 498 39. Kerkoerle T, Self MW and Roelfsema PR. (2017) Layer-specificity in the effects of  
499 attention and working memory on activity in primary visual cortex. *Nature*  
500 *Communications*, **8**: e13804. <http://doi.org/10.1038/ncomms13804>
- 501 40. Lake BB, Ai R, Kaeser GE, Salathia NS, Yung YC, Liu R, Wildberg A, Gao D, Fung H-L,  
502 Chen S, Vijayaraghavan R, Wong J, Chen A, Sheng X, Kaper F, Shen R, Ronaghi M, Fan  
503 J-B, Wang W, Chun J, Zhang, K. (2016) Neuronal subtypes and diversity revealed by  
504 single-nucleus RNA sequencing of the human brain. *Science*, **352**(6293): 1586–1590.  
505 <http://doi.org/10.1126/science.aaf1204>
- 506 41. Krauzlis RJ, Bollimunta A, Arcizet F, Wang L. (2014) Attention as an effect not a cause.  
507 *Trend Cog Sci*, **18**(9): 457–464. <http://doi.org/http://dx.doi.org/10.1016/j.tics.2014.05.008>
- 508 42. Jeannerod M. (2006) *Motor Cognition*. Oxford University Press. ISBN: 0198569653
- 509 43. Koch C and Tsuchiya N. (2007) Attention and consciousness: two distinct brain processes.  
510 *Trends in Cognitive Sciences*, **11**(1): 16–22. <http://doi.org/10.1016/j.tics.2006.10.012>
- 511 44. Boxtel JJA, Tsuchiya N and Koch C. (2010) Consciousness and attention: on sufficiency  
512 and necessity. *Frontiers in Psychology*, **1**: e217. <http://doi.org/10.3389/fpsyg.2010.00217>
- 513 45. Vandierendonck A. (2014) Symbiosis of executive and selective attention in working  
514 memory. *Frontiers in Hum Neurosci*, **8**: E588. <http://doi.org/10.3389/fnhum.2014.00588>
- 515 46. Quak M, London RE and Talsma D. (2015) A multisensory perspective of working  
516 memory. *Frontiers in Hum Neurosci*, **9**: E197. <http://doi.org/10.3389/fnhum.2015.00197>
- 517 47. Royall DR and Palmer RF. (2014) “Executive functions” cannot be distinguished from  
518 general intelligence: two variations on a single theme within a symphony of latent  
519 variance. *Frontiers in Behav Neurosci*, **8**: E369. <http://doi.org/10.3389/fnbeh.2014.00369>
- 520 48. Lucenet J and Blaye A. (2014) Age-related changes in the temporal dynamics of executive  
521 control: a study in 5- and 6-year-old children. *Frontiers in Psychology*, **5**: E831.  
522 <http://doi.org/10.3389/fpsyg.2014.00831>

- 523 49. Burkart JM, Schubiger MN and Schaik CP. (2016) The evolution of general intelligence.  
524 *Behavioral and Brain Sci*, **Jul 28**: 1–65. <http://doi.org/10.1017/S0140525X16000959>
- 525 50. Pal NR, Bezdek JC, and Hathaway RJ. (1996) Sequential Competitive Learning and the  
526 Fuzzy *c*-Means Clustering Algorithms. *Neural Networks*, **9**(5): 787–796.
- 527 51. Belgard TG, Marques AC, Oliver PL, Abaan HO, Sirey TM, Hoerder-Suabedissen A,  
528 García-Moreno F, Molnár Z, Margulies EH, Ponting CP. (2011) A Transcriptomic Atlas  
529 of Mouse Neocortical Layers. *Neuron*, **71**(4): 605–616.  
530 <http://doi.org/10.1016/j.neuron.2011.06.039>
- 531 52. Yaguchi K, Nishimura-Akiyoshi S, Kuroki S, Onodera T, Itohara S. (2014) Identification  
532 of transcriptional regulatory elements for *Ntng1* and *Ntng2* genes in mice. *Molecular*  
533 *Brain*, **7**(1): 19. <http://doi.org/10.1186/1756-6606-7-19>